INTERNATIONAL JOURNAL OF OPTIMIZATION IN CIVIL ENGINEERING
Int. J. Optim. Civil Eng., 2022; 12(3):411-433

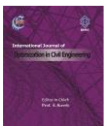

SEISMIC ENERGY DEMANDS OF INELASTIC BUILDINGS DESIGNED WITH OPTIMUM DISPLACEMENT-BASED APPROACH

B. Ganjavi[1*, †] and M. Barania[2]
[1]*Department of Civil Engineering, University of Mazandaran, Babolsar, Iran*
[2]*Department of Civil, Water & Environmental Engineering, Shahid Beheshti University, Tehran, Iran*

ABSTRACT

In present study, the effects of optimization on seismic energy spectra including input energy, damping energy and yielding hysteretic energy are parametrically discussed. To this end, 12 generic steel moment-resisting frames having fundamental periods ranging from 0.3 to 3s are optimized by using uniform damage and deformation approaches subjected to a series of 40 non-pule strong ground motions. In order to obtain the optimum distribution of structural properties, an iterative optimization procedure has been adopted. In this approach, the structural properties are modified so that inefficient material is gradually shifted from strong to weak areas of a structure. This process is continued until a state of uniform damage is achieved. Then, the maximum energy demand parameters are computed for different structures designed by optimum load pattern as well as code-based pattern, and the mean energy spectra, energy-based reduction factor and the dispersion of the results are compared and discussed. Results indicate that optimum seismic load pattern can significantly affect the energy demands spectra especially in inelastic range of response. In addition, using energy-based reduction factors of optimum structures in short-period and long-period regions will result in respectively overestimation and underestimation of the required input energy demands for code-based structures, reflecting the difference dose exists in reality between the conventional forced-based methodology and energy-based seismic design approach that can more realistically incorporate the frequency content and duration of earthquake ground motions.

Keywords: Energy demand spectra; Optimum design; nonlinear dynamic analysis; performance-based approach, statistical analysis, Inelastic behavior.
Received: 10 March 2022; Accepted: 20 April 2022

[*]Corresponding author: Department of Civil Engineering, University of Mazandaran, Babolsar, Iran
[†]E-mail address: b.ganjavi@umz.ac.ir (B. Ganjavi)

1. INTRODUCTION

When building structures are properly designed against earthquakes, the property damages and related fatalities are substantially reduced. Currently, seismic design procedures stipulated in earthquake design codes such as ASCE-7-16 [1] and IBC-2015 [2]; Erocode-8 [3] and Iranian Code of Practice, Standard No. 2800 [4] are widely used by practicing engineers to design structures that can resist earthquake forces with an acceptable damage, which is referred to as damage levels in performance-based design codes such as FEMA 356 [5]. Forced-based and displacement-based design approaches are two of the widely used conventional performance-based design procedures in the world. The fundamental concept of these procedures are based on nonlinear static (pushover) methods. In the force-based seismic design (FBSD) method, a design lateral force for a given structure is computed based on an elastic design acceleration response spectrum, which is called the design base shear. To consider the inelastic behavior, the design shear force of a given structural system obtained from the elastic acceleration response spectrum is reduced by a strength-reduction factor or so-called response modification factor. The structure is then designed for the reduced shear strength, and the displacement or inter-story drift can be controlled so that the code-compliant limits are coped with. However, many limitations and drawbacks have been reported by researchers on the FBSD procedure. In one of the detailed investigations, Smith and Tso [6] through studying on a large family of reinforced-concrete members such as flexural walls, piers and ductile moment-resisting fames asserted that force-based seismic design procedure is inconsistent. They concluded that the assumption of the independency of the shear strength and shear stiffness of a lateral load resisting system is essentially inconsistent since they are indeed related and proportional. Instead of using design base shear as in the case for FBSD, the displacement-based seismic design (DBSD) method, in general considered to be a better substitute for the FBSD approach, takes inter-story drift or displacement in the design process. Consequently, the key task in a DBSD method is to estimate the maximum displacement demand in a given structure with rational accuracy and simplicity as a function of its local mechanical properties including element deformation and strain limits. One of the currently available DBSD methods is the Displacement-Based Coefficient Method (DBCM) provided by FEMA 440 [7]. In this method the linear elastic response of an equivalent SDOF (E-SDF) system is modified by multiplying it by a series of coefficients to compute a target (global) displacement. This approach utilizes an idealized pushover curve corresponding to a given damping ratio of base shear strength with respect to roof displacement developed for a real MDOF structure. The accuracy of the DBSD procedure is highly dependent on how closely the equivalent SDOF system and its MDOF counterpart are related through the idealized pushover curve. Recently, researchers have identified some drawbacks in the use of roof displacement-based pushover curve. As an instance, Hernandez-Montes *et al.* [8] pointed out that the use of roof displacement in producing the capacity curve would be confusing since the capacity curve occasionally tends to exhibit the structure as a source of energy rather than absorbing energy. Neither the FBSD procedure, using base shear strength as a design parameter, nor the DBD method, using displacement as a design parameter, can directly account for the cumulative damage influence that result from several inelastic cycles of the earthquake ground motion due to

strength and stiffness deterioration of the structural hysteretic behavior. As a result, the effect of earthquake excitation on structural systems should be interpreted not only just as a force or displacement quantity, but also as a product of both aforementioned parameters which can be described in terms of energy. This is the underlying concept for the inception of the energy-based seismic design (EBSD) approach, which is suggested by many researchers to be considered as the next generation of seismic design procedures.

It is believed that a more rational seismic design approach is to express the dynamic input effect through energy response spectra. Interpreting the effect of earthquakes in terms of energy is gaining extensive attention [9-23]. This approach has three major advantages: (i) the input effect in terms of energy and the structural resistance in terms of energy dissipation capacity are basically uncoupled, (ii) except in the short period range, the input energy introduced by a given ground motion in a structure is a stable quantity, governed primarily by the fundamental natural period and the mass, and scarcely by other structural properties such as resistance, damping and hysteretic behavior, and (iii) the consideration of the cumulative damage fits well with this formulation and can be directly addressed. In the energy-based methods the design criterion is constituted by the comparison between the energy absorption capacity of the structure (i.e. its seismic resistance) and the input energy (i.e. the effect of the ground motion). It is then necessary to establish the input energy spectrum corresponding to the expected earthquake, i.e. design input energy spectrum. On the other hand, it is also well known that structural characteristics in terms of stiffness and strength distributions have a key role in seismic demands of structures. In a comprehensive parametric study, Ganjavi and Hao [24] through intensive parametric analyses of 21600 linear and nonlinear MDOF systems and considering five different shear strength and stiffness distribution patterns subjected to a group of earthquakes recorded on alluvium and soft soils, the effect of structural lateral stiffness and strength distribution on strength demand and ductility reduction factor spectra of MDOF fixed-base and soil-structure systems were parametrically investigated. Results of this study showed that depending on the level of inelasticity, soil flexibility and number of degrees-of-freedoms (DOFs), structural characteristics distribution can significantly affect the strength demand and ductility reduction factor of MDOF systems. In this regard, several studies have been conducted by researchers to evaluate and improve the code-specified design lateral load patterns of fixed-base systems based on the inelastic behavior of the structures [25-29]. More recently, an optimization procedure have been performed for soil-structure system taken into consideration of superstructure elastic and inelastic behaviors [30-31]. However, the effect of optimum seismic design and load patterns on seismic energy demands of building structures have not been well addressed yet. It is in this area that the present study attempts to make a contribution. In this study, steel moment-resisting frames are optimized by using uniform damage and deformation approaches subjected to a series of strong ground motions. Then, the maximum energy demand parameters are computed for different structures designed by optimum load pattern as well as code-based pattern. The effect of optimization on seismic energy spectra including input energy, damping energy and hysteretic energy are parametrically discussed.

2. SIMPLIFIED GENERIC MOMENT-RESISTING FRAME PROTOTYPES AND EARTHQUAKE EXCITATIONS

During the past twenty years, different types of simplified generic frames have been introduced and developed by many researchers for evaluating seismic response and behavior of steel and concrete moment-resisting frames. In geometry viewpoint, generic frames used in the past can be divided into two main categories: (a) fishbone-shape generic frames (b) single-bay generic frames, and (2). “Fishbone” shape generic frames are a type of generic frame utilized by Ogawa et. al. [32], Luco et. al., [33], Nakashima et. al [34], and Kahloo and Khosravi [35]. In this simple model, a multi-bay frame can be modeled as a cantilever beam with two rotational springs at each floor level connected to roller supports on each side of the cantilever. One of the main assumptions in the development of this type of generic frames is existing the identical rotations of joints at the same floor. As with the second type of generic frame, many researches such as those conducted by Medina and Krawinkler [36], Esteva and Ruiz [37] and Park [25] showed that the response of a multi-bay building can be simulated adequately by a single-bay frame. This approach has attracted researchers for seismic performance assessment since it represents a less computational effort for performing repeated nonlinear dynamic time history analyses. Results obtained by the researchers demonstrated that single-bay generic frame models are adequate to represent the global dynamic behavior of more complex regular multi-story frames exposed to earthquake excitations [38-39]. In this study the single-bay steel frame reprehensive of steel moment resisting frame structures are utilized for parametric study. A schematic shape of the generic frame is shown in Fig. 1. The generic frame prototypes used in this study are 12 single-bay, steel frames with the number of stories ranging from three to twenty. The fundamental periods are 0.3, 0.4, 0.6, 0.8, 1.0, 1.2, 1.5, 1.8, 2.1, 2.4, 2.7 and 3.0 s. The main properties of the generic frames used in this paper are as follows:

(1) Models are two-dimensional steel moment-resisting frames. The distribution of story mass is uniform over the floor levels. For all generic frames, story height is constant and equal to 3.6 m. Moreover, the beam span is equal to 7.2 m.
(2) The effect of finite joint regions is not taken into account, meaning the dimensions of centerline are considered for column and beam members.
(3) The generic frames are designed based on the strong column-weak-beam (SCWB) concept. In other words, the plastic hinge is confined only at the beam ends and at the bottom of the first story columns as shown in Fig 1.
(4) When the frame is undergone to a given lateral load pattern, the same value of over-strength is supposed at all stories, which means that beams and columns strengths are adjusted such that yielding occurs simultaneously at all plastic hinge locations. This provides the computation of inter-story ductility ratio which in its turn is obtained from yield story drift.
(5) The first mode shape for all the models is a straight-line, which regards to the fact that each story stiffness is adjusted so that as the frame is under a triangular load pattern, a uniform height-wise distribution of story drifts over the height is occurred. In this manner, the relative height-wise distribution of member stiffness along the height is also achieved.

(6) The P-Delta for the whole structure which is called as global effect is considered through quantifying the elastic first story stability coefficient as proposed by Medina and Krawinkler (2005), whereas member P-Delta is not taken into account for.
(7) In time history dynamic analysis, structural damping is modelled based on Rayleigh damping model with 5% of critical damping assigned to the first mode as well as to the mode where the cumulative mass participation is at least 95%.
(8) The moment-rotation hysteretic behavior is modeled by using rotational springs with Modified-Clough stiffness degrading model with 2% strain hardening (Fig. 2).
(9) In addition, Modified Rayleigh-type damping model for proper modeling of structural damping in inelastic plane structural systems proposed by Zareian and Medina [40] was utilized to have more reliable results in time history analysis.

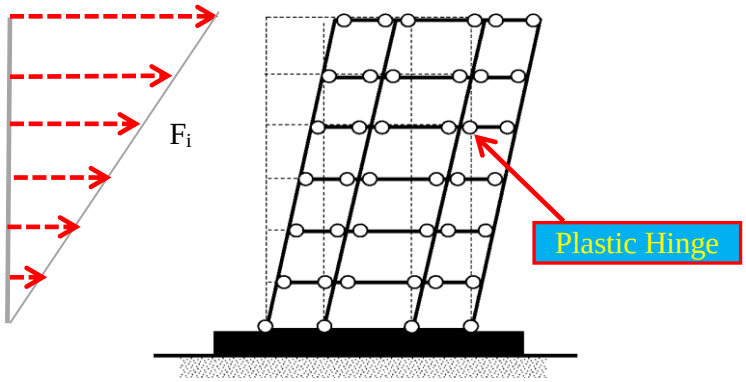

Figure 1. Schematic generic steel moment-resisting frame used in this study

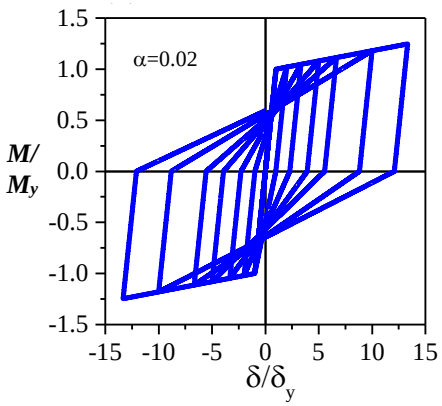

Figure 2. Modified clough stiffness degrading model

For nonlinear dynamic analyses a set of 40 ground motions located on alluvium soil site deposits was compiled from six strong earthquakes recorded on soil type III on Iranian seismic code [4]. They were selected from strong ground motion database of the Pacific Earthquake Engineering Center (PEER). These earthquake ground motions have been selected based on the given assumptions including: (a) They exclude the near-fault ground motion characteristic such as pulse type and forward directivity effects. The effect of near-

fault ground motions on structures is more pronounced compared to that of far-fault ones. The distinct effects of near-fault earthquake ground motions require to be assessed separately during the design process, and the result of a study based on a combination of near-fault and far-fault ground motion records is likely to give misleading conclusions. Consequently, this study has excluded near-fault ground motion records in the selected ground motion ensemble and is primarily focused on far-fault ground motion effects. (b) They are not located on soft soil profiles; hence the effect soil-structure interaction has not been considered in this study (c) They have no long duration characteristics. (d) The selected earthquake ground motions have moment magnitude equal or larger than 6.5 covering ground motions referred to as strong to major earthquakes, and closest distance to the fault rupture is less than 40 km. (e) These ground motions are recorded on soils that correspond to IBC-2015 site class D, which is approximately similar to the soil type III of the Iranian seismic code of practice, Standard No. 2800 [4]. (f) These ground motions have been scaled based on ASCE7-16 [1] to be consistent with those that dominate the 10 percent probability of exceedance of a given ground motion intensity measure in 50 years. The main properties of ground motion are provided in Table 1.

Table 1: Ground motions used in this study

Event	Year	Station	*Mw*	*R* (km)	PGA (g)	PGV (cm/s)	D^a (s)	L^b (s)
Imperial Valley	1979	Calipatria Fire Station	6.5	23.8	0.078	13.3	23.3	39.5
Imperial Valley	1979	Chihuahua		28.7	0.270	24.9	20.1	40.0
Imperial Valley	1979	Compuertas		32.6	0.186	13.9	21.7	36.0
Imperial Valley	1979	El Centro Array #1		15.5	0.139	16.0	8.9	39.5
Imperial Valley	1979	El Centro Array #12		18.2	0.116	21.8	19.4	39.0
Imperial Valley	1979	El Centro Array #13		21.9	0.139	13.0	21.2	39.5
Imperial Valley	1979	Niland Fire Station		35.9	0.109	11.9	21.7	40.0
Imperial Valley	1979	Plaster City		31.7	0.057	5.4	10.7	18.7
Imperial Valley	1979	Cucapah		23.6	0.309	36.3	15.7	40.0
Imperial Valley	1979	Westmorland Fire Station		15.1	0.110	21.9	25.2	40.0
Loma Prieta	1989	Agnews State Hospital	6.9	28.2	0.172	26.0	18.4	40.0
Loma Prieta	1989	Capitola		14.5	0.443	29.3	13.2	40.0
Loma Prieta	1989	Gilroy Array #3		14.4	0.367	44.7	11.4	39.9
Loma Prieta	1989	Gilroy Array #4		16.1	0.212	37.9	14.8	39.9
Loma Prieta	1989	Gilroy Array #7		24.2	0.226	16.4	11.5	39.9
Loma Prieta	1989	Hollister City Hall		28.2	0.247	38.5	17.4	39.1
Loma Prieta	1989	Hollister Differential Array		25.8	0.279	35.6	13.2	39.6
Loma Prieta	1989	Halls Valley		31.6	0.134	15.4	16.2	39.9
Loma Prieta	1989	Salinas—John and Work		32.6	0.112	15.7	20.3	39.9
Loma Prieta	1989	Palo Alto—SLAC Lab.		36.3	0.194	37.5	12.5	39.6
Loma Prieta	1989	Sunnyvale—Colton Ave.		28.8	0.207	37.3	21.2	39.2
Northridge	1994	LA—Centinela St.	6.7	30.9	0.322	22.9	12.4	30.0
Northridge	1994	Canoga Park—Topanga Can.		15.8	0.420	60.8	10.4	25.0

Northridge	1994	LA—N Faring Rd.		23.9	0.273	15.8	8.8	30.0
Northridge	1994	LA—Fletcher Dr.		29.5	0.240	26.2	11.8	30.0
Northridge	1994	Glendale—Las Palmas		25.4	0.206	7.4	11.5	30.0
Northridge	1994	LA—Hollywood Stor FF		25.5	0.231	18.3	12.0	40.0
Northridge	1994	Lake Hughes #1		36.3	0.087	9.4	13.9	32.0
Northridge	1994	Leona Valley #2		37.7	0.063	7.2	12.5	32.0
Northridge	1994	Leona Valley #6		38.5	0.178	14.4	10.4	32.0
Northridge	1994	La Crescenta—New York		22.3	0.159	11.3	11.0	30.0
Northridge	1994	LA—Pico and Sentous		32.7	0.186	14.3	14.8	40.0
Northridge	1994	Northridge—17645 Saticoy St.		13.3	0.368	28.9	15.7	30.0
Northridge	1994	LA—Saturn St.		30.0	0.474	34.6	11.6	31.6
Northridge	1994	LA—E.Vernon Ave.		39.3	0.153	10.1	15.9	30.0
San Fernando	1971	LA—Hollywood Stor Lot	6.6	21.2	0.174	14.9	11.2	28.0
Superstition Hills	1987	Brawley	6.7	18.2	0.156	13.9	13.5	22.1
Superstition Hills	1987	El Centro Imp. Co. Cent		13.9	0.358	46.4	16.1	40.0
Superstition Hills	1987	Plaster City		21.0	0.186	20.6	11.3	22.2
Superstition Hills	1987	Westmorland Fire Station		13.3	0.172	23.5	19.6	40.0

[a]Duration of strong motion (defined as the time it takes for the cumulative energy of the ground motion record to grow from 5 to 95% of its value at the end of the history).

[b]Length of record

3. METHODOLOGY FOR COMPUTING THE SEISMIC ENERGY DEMANDS OF STRUCTURES BASED ON OPTIMUM DISPLACEMENT-BASED METHOD

As indicated in the literature, seismic load pattern can have significant effect on seismic response of the structures. To investigate this effect from energy point of view, a methodology for computing the energy demand spectra of optimized steel moment-frame prototypes is proposed. Optimum-designed steel moment frame models are regarded as the structure in which the story structural damage (i.e., deformation or ductility demand) are distributed uniformly along the height of a the frame under a given earthquake excitation. The required relative shear strength pattern corresponding to this performance target is called optimum lateral load pattern which can be compared with the code-compliant design lateral load patterns [2, 4]. In such a case, based on the step-by-step procedure presented in this study, one can easily compare the required elastic and inelastic energy demands spectra of the code-based and optimum designed frame prototypes when subjected to a family of realistic earthquake ground motion excitations. In this regard, it is essential to select proper engineering response or demand parameters to determine the optimum distribution of the structural damage over the height. Among them, inter-story and global ductility ratios, maximum inter-story drift ratio, the number of cycles of yielding, cyclic story ductility and also a combination of above-mentioned parameters are those of such engineering demand parameters that are commonly used by researches to compute seismic damage imparted to a structure [26, 36, 41-42]. Two of the aforementioned parameters widely used by many

researchers to quantify the structural damage for non-deteriorating structural systems are the maximum inter-story drift ratio defined as the maximum relative displacement between two consecutive story levels normalized by the story height. In addition, the inter-story ductility ratio (μ_i) in *i*-th story is defined as the difference between the maximum inter-story drift angle $(\alpha_{\max})_i$ and the inter-story yield drift angle $(\alpha_y)_i$ normalized by the inter-story yield drift angle. Generally, a steel structure with ductile structural elements with no strength deterioration can withstand forces and carry larger loading without losing its carrying capacity entirely. In performance based-seismic design, the maximum story drift and ductility ratios are two of the most appropriate parameters to determine the structural damage. It is believed that they have several advantages such as (i) they are very simple parameters to be computed by researchers; (ii) they are perceptible for all structural engineers; and (iii) many experimental studies have been carried on these parameters. Therefore, they can be considered as sufficient earthquake engineering demand parameters to evaluate the structural damage imparted to the building structures during an earthquake event. in this study, these parameters are selected as suitable indicators of structural damage. Although, different optimization algorithms have been proposed by researches such as those recently developed by Kaveh [43], based on the parameters used in this study the following practical step-by-step iteration process is proposed for the generic steel frame models introduced in previous sections under a given earthquake ground motion to achieve optimum-designed energy demands spectra:

1. Select a frame prototype with the target fundamental period (T_1) and specific number of stories. Calculate and assign member stiffness based on the first mode shape of shear-type structure through pushover analysis. An iteration process should be conducted to achieve a presumed fundamental period of vibration.
2. Consider the target inter-story ductility ratio, μ_t, and perform nonlinear pushover analysis and assign member strengths based on an arbitrary seismic design lateral force pattern such as code-based pattern. In this investigation, for nonlinear static pushover and non-linear time history dynamic analyses, the computer program OpenSees [44] developed at the University of Berkeley is utilized. The solutions are obtained using step-by-step integration of equations of motion using Newmark beta method.
3. Select and scale a given ground motion based on seismic code ([1] or [2]) for the desired hazard level. Here, the ground motion hazard level with 10 percent probability of exceedance of a given ground motion intensity measure in 50 years is selected.
4. Perform nonlinear dynamics time history analysis and calculate the maximum inter-story ductility ratio, $\mu_{\max(i)}$. Control the ductility demand such that the following expression is achieved.

$$\beta_i = \left| \frac{\mu_{\max i} - \mu_t}{\mu_t} \right| \times 100 \le 0.5 \tag{1}$$

If the above condition is met, the structure will be regarded as optimum. Otherwise, the story shear strength at each story must be modified by a correction factor of $(\mu_{\max i}/\mu_t)^{0.05}$. The process of updating the height-wise distribution of story shear strength is repeated until

β_i is less than 0.5.

5. The designed frame is optimum and energy demand parameters need to be computed.

For MDOF systems the governing equation of the motion subjected to a horizontal earthquake ground motion can be defined as:

$$[M]\left[\ddot{u}(t)\right]+[C]\left[\dot{u}(t)\right]+[K]\left[u(t)\right]=-[M]\left[\ddot{u}_g(t)\right] \tag{2}$$

where M, C, and K are mass, damping, and lateral stiffness matrices of the system, respectively. $\ddot{u}(t)$ is the relative acceleration, $\dot{u}(t)$ is the relative velocity, $u(t)$ is the vector of *i*-th lateral floor displacements relative to the ground with *t* representing time, $\ddot{u}_g(t)$ is vector of the ground acceleration [45]. By integrating Eq. (2), the energy equation of an MDOF system can be obtained:

$$\int_0^t M\left[\ddot{u}(t)\right]+\int_0^t C\left[\dot{u}(t)\right]+\int_0^t [K]\left[u(t)\right]=-\int_0^t [M]\left[\ddot{u}_g(t)\right] \tag{3}$$

In another form, the Eq. (3) can be written as:

$$\int_0^t M\ddot{u}_t(t)du+\int_0^t C\dot{u}(t)du+\int_0^t Ku(t)du=0 \tag{4}$$

where $\ddot{u}_t=\ddot{u}+\ddot{u}_g$. For a diagonal matrix of M, the Eq.[4] can be written as:

$$E_K(t)+E_D(t)+E_H(t)=E_I(t) \tag{5}$$

where

$$E_K(t)=\frac{1}{2}\sum_{i=1}^{n} m_{ii}\dot{u}_{ti}^{\,2}(t) \tag{6}$$

$$E_D(t)=\int_0^t[\sum_{i=1}^{n}\sum_{j=1}^{n} c_{ij}\dot{u}_i(t)\dot{u}_j(t)]dt \tag{7}$$

$$E_A(t)=\int_0^t[\sum_{i=1}^{n}\sum_{j=1}^{n} k_{ij}u_i(t)\dot{u}_j(t)]dt \tag{8}$$

$$E_I(t)=\int_0^t\sum_{i=1}^{n} m_{ii}\ddot{u}_{ti}(t)\dot{u}_g(t)dt \tag{9}$$

where $E_K(t)$, $E_D(t)$ are respectively is absolute kinetic energy, damping energy. $E_A(t)$ is retrievable absorbed energy due to elastic strain and hysteretic energy $E_h(t)$ that is unrecoverable and is directly related to the yielding of the structural elements, $E_I(t)$ is the total absolute input energy of the system, and m, c, and k represent the components of matrices M, C, and K, respectively. For a nonlinear system with concentrated plasticity, Eqs. (7-8) for computing time history energy demand parameters can be written as:

$$E_D\left(t_f\right)=\sum_{t=0}^{t_f}\left(\sum_{i=1}^{n}\sum_{j=1}^{n}c_{ij}\left(t\right)\dot{u}_i\left(t\right)\dot{u}_j\left(t\right)\right)\Delta t \tag{10}$$

$$E_A\left(t_f\right)=\frac{1}{2}\sum_{i=1}^{n}\sum_{j=1}^{n}K_{ij}\left(t\right)u_i\left(t\right)u_j\left(t\right) \tag{11}$$

$$E_I'\left(t_f\right)=\sum_{t=0}^{t_f}\left(\sum_{i=1}^{n}m_{ii}\ddot{u}_g\left(t\right)\dot{u}_i\left(t\right)\right)\Delta t \tag{12}$$

where t_f and Δt are time step in dynamic analysis and total ground motion duration.

6. Having $\ddot{u}_g(t)$, $\dot{u}(t)$ and $u(t)$ from the optimum designed structure obtained from step 5, the time history energy demands are computed from Eqs (10) to (12).
7. Steps 1- 6 are repeated for optimum and code-based designed structures of other models with different number of stories, fundamental periods, ductility ratios (i.e., μt= 2,3,4,6), to obtain the input, damping and hysteretic energy demands spectra.

The proposed optimization method is applied to a generic steel frame of 12 stories with T= 1.5 sec, and μt= 2 and 6 representing low and high levels of inelasticity subjected to 40 earthquake ground motions used in this study. Table 2 shows a comparison of the average results obtained from optimum designed structures and the corresponding code-compliant designed models. It can be seen that a significant difference is observed between the story damage distribution (ductility demand profiles) resulted from the two designed frames. In fact, the height-wise distributions of story ductility demands resulted from utilizing code-based design lateral load patterns [1] are very non-uniform with respect to the corresponding optimum cases. As seen from Table 2, the coefficient of variation (COV) for ductility demand distributions in optimum designed structures are significantly lower than those in code-based structures.

Table 2: Mean story ductility demands for 12-story optimum and code-based designed frames

	μ=2		μ=6	
Story	μ_{Code} **COV= 42.7%**	μ_{OPT} **COV= 1.18%**	μ_{Code} **COV= 54.2%**	μ_{OPT} **COV= 2.1%**
1	1.00	2.02	6.01	6.02
2	0.90	1.98	5.14	5.95
3	0.75	1.97	4.42	5.9
4	0.72	1.96	3.75	5.93

5	0.62	1.95	3.17	5.85
6	0.66	1.98	2.83	5.88
7	0.67	1.95	1.77	6.02
8	0.72	1.99	1.51	6.03
9	0.90	1.96	1.29	5.94
10	1.20	1.97	1.14	5.89
11	1.50	1.94	1.42	5.88
12	2.00	2	3.95	5.87

4. SEISMIC ENERGY DEMANDS OF BUILDING STRUCTURES DESIGNED BASED ON OPTIMUM DISPLACEMENT-BASED AND CODE-BASED LOAD PATTERNS

To investigate the effect of optimum deformation theory on energy demands spectra, the proposed optimization algorithm are applied and energy demand parameters defined through Eqs. (10) to (12) were computed for all of the 12 generic-framed steel-moment resisting systems with the fundamental periods of vibration ranging from 0.3 to 3.0 s, for four levels of inelastic behaviors μ= 2, 3, 4, 6, representing the low, moderate, high and severe inelastic states, respectively. However, for input energy demand spectra the elastic state was also depicted. Fig. 3 shows the mean results for input energy, damping energy and yielding hysteretic energy spectra subjected to 40 earthquake ground motions. In order to compare the results, all the energy parameters which are shown in the vertical axis of the provided figure are normalized by total building mass. The abscissa in all figures is also the fundamental period of vibration of structures. In Fig. 3, the plots in the left side correspond to the optimum design (denoted by OPT_UDT) and the plots in the right side correspond to the code-based structures designed by seismic code patterns (denoted by SCP). As can be seen in input energy spectra, the general form of the code-based and optimum structures are identical. Nevertheless, in inelastic range of response, the average energy demand imparted to the mid- and long-period code-based frames are greater than those imparted to the corresponding optimum models. This phenomenon will be discussed in more detail in the next part. Normalized damping energy spectra of code-based and optimum frame prototypes also show the same variation as illustrated for input energy spectra. However, the damping energies of the optimum structures are significantly lower than those of the code-based structures, which is more significant for higher inelastic range of responses. In addition, it is observed that the variation of normalized damping energy demands with ductility ratio (μ) for code-based frames is more sensitive than optimum designed structures such that in comparison to optimum structures, as ductility ratio increases the damping energy decreases with greater quantities. The general trend of normalized hysteretic energy spectra are somewhat different from input and damping energy spectra such that in code-based designed structures by increasing the inelastic behavior the hysteretic energy demands significantly increase while for the cases of optimum structures, except for low inelastic state with μ= 2, no substantial variations can be seen for moderate and high inelastic behaviors. In addition,

unlike to the input and damping energy spectra, the mean values of hysteretic energy demand for optimum structures are significantly larger than those of corresponding structures designed by code-based patterns, which are more pronounced for low level of inelastic behavior. This phenomenon indicates that in optimum structures the seismic energy dissipation in each structural element is maximized and the material capacity is fully exploited. For better understanding, the ratios of damping and hysteretic energies to the corresponding input energy for different inelastic behaviors are computed and the mean results are depicted in Figs. 4 and 5. Results show that the damping energy ratios for optimum structures are always lower than code-based structures, whereas the trend is reversed for the case of hysteretic energy ratios. Moreover, it can be seen that, regardless of inelastic level of response, the damping and hysteretic energy ratios for both code-based and optimum strictures are in average independent of fundamental period of vibration. Therefore, the ratios can be considered only a function of target inter-story ductility demands of structures.

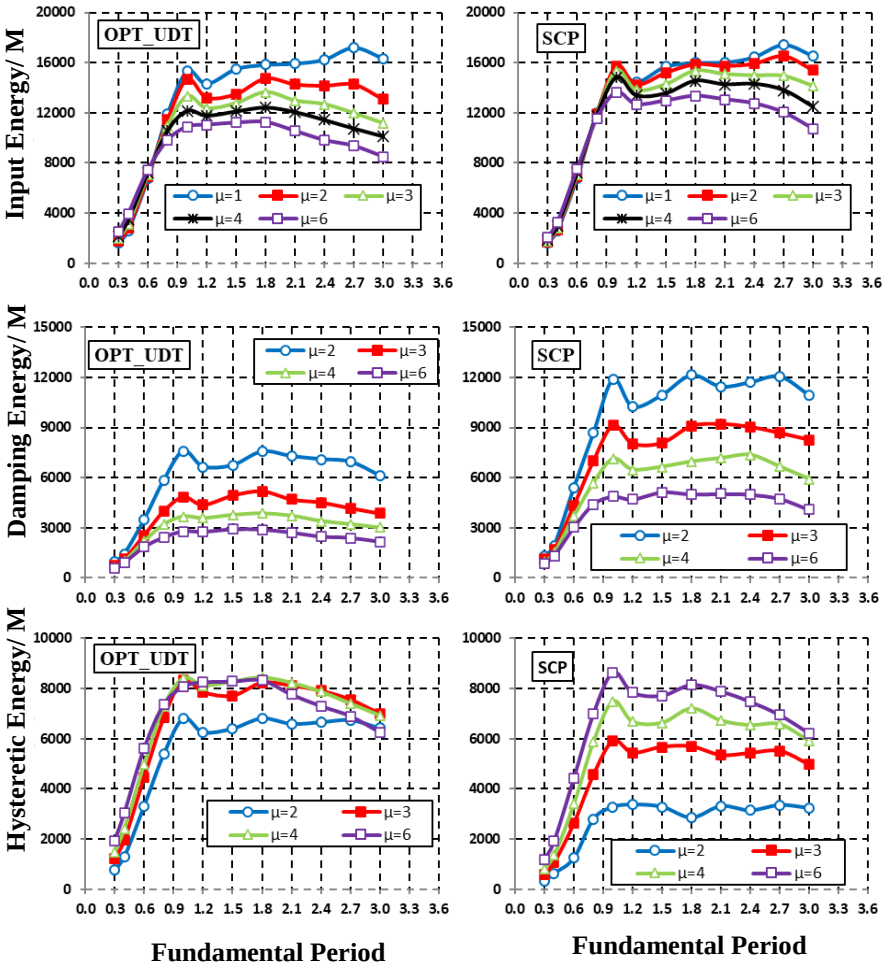

Figure 3. Normalized spectra of energy parameters for optimum pattern (left) and code-based design pattern (Right); average of 40 earthquakes

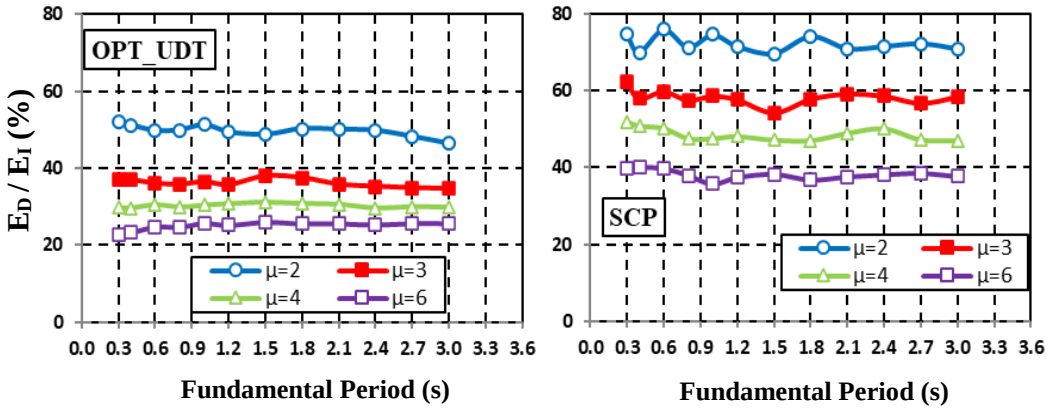

Figure 4. Normalized spectra of energy parameters for optimum pattern (left) and code-based design pattern (Right); average of 40 earthquakes

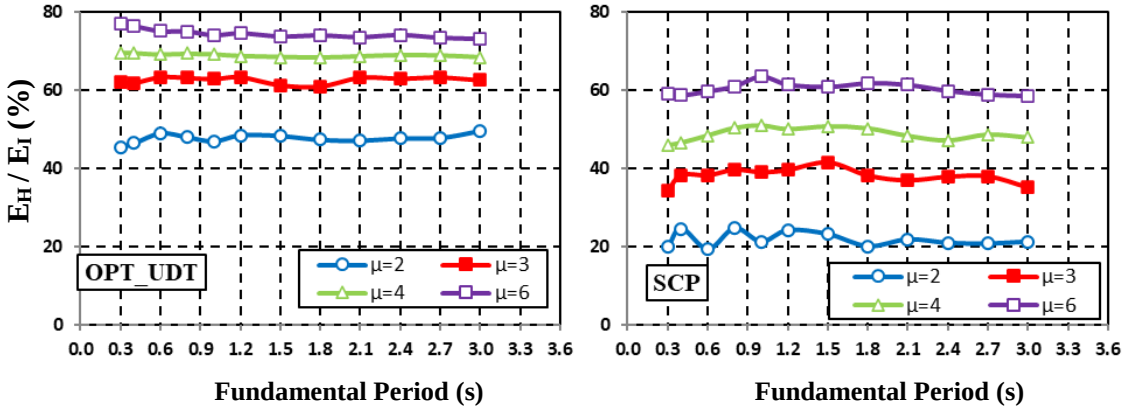

Figure 5. Normalized spectra of energy parameters for optimum pattern (left) and code-based design pattern (Right); average of 40 earthquakes

To more precisely investigate the effect of optimum seismic design load patterns on energy demand parameters Fig. 6 is provided. The vertical axis in the this figure shows the ratios of energy parameters in optimum structures to those in corresponding code-based designed structures which are defined as:

$$E_I Ratio = \frac{(E_{1\max} / M)_{OPT}}{(E_{1\max} / M)_{SCP}} \tag{13}$$

$$E_H Ratio = \frac{(E_{D\max} / M)_{OPT}}{(E_{D\max} / M)_{SCP}} \tag{14}$$

where $E_I Ratio$, $E_D Ratio$ and $E_H Ratio$ are input energy, damping energy and hysteretic energy ratios, respectively. By observing the Fig.(6-a), it is found that in elastic range of response (μ=1), $E_I Ratio$ is in average independent of seismic load pattern, and optimization does not

affect the elastic energy demand imparted to the structures. Nevertheless, when structures inter to the inelastic state, this ratio is remarkably influenced by the variation of the ductility ratio such that in short-period structures the energy values imparted to the optimum structures are larger (up to 21%) than those imparted to the code-based systems. After a threshold period (here T=0.6), the trend is reversed in such a way that the optimum designed structures take the input energies much lower than the corresponding code-based models, which are more intensified as the target ductility ratio increases i.e., up to 23% less than code-based frames, signifying the effect of seismic load patterns on seismic input energy demands of MDOF structures. Therefore, using the displacement-based optimum design philosophy can result in overestimation and underestimation of input energy demands for the structures designed based code-compliant lateral load patterns. Similar to the $E_I Ratio$, Figs. (6-b) and (6-c) are illustrated for $E_D Ratio$ and $E_H Ratio$. Considering Fig. (6-b), it is obvious that for all ductility ratios the values of $E_D Ratio$ are always less than unity, meaning that the damping energy in optimum structures are always lower than code-based structures. This conclusion is in accordance to the optimization target which indicates that a status of uniform distribution of structural damage over the height of the structures is a direct outcome of the optimum use of material. In fact, it is expected that the dissipation of seismic energy in each element is maximized and the material capacity is fully exploited, which is observable in Fig. (6-c). As seen, the values of $E_H Ratio$ are always significantly larger than unity, implying that the optimum structure can dissipate the seismic input energy through inelastic behavior of their structural elements much more than its code-based designed structure counterpart. The maximum ratio is 2.56 for low inelastic behavior and reaches 1.2 for μ=6. The interesting point is that while the input energy demands of optimum structures are generally greater than code-based structures, the structural weight in optimum frames is much lower than that in structures designed by seismic code load pattern (see Fig. 7). It is seen that as ductility demand increases the structural weight ratio, defined as structural weight in code-based structures normalized by structural weight in the corresponding optimum structure (denoted by ψ), increases up to 2.2 for higher level inelastic behavior, demonstrating the efficiency of the proposed optimization approaches in seismic performance of building structures.

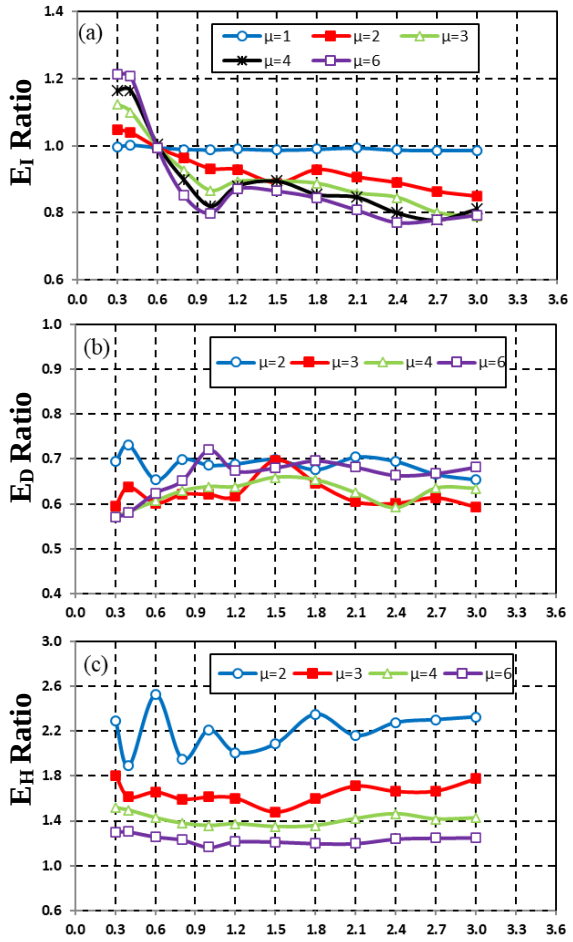

Figure 6. (The ratio of OPT to Code) Normalized spectra of energy parameters for optimum pattern (left) and code-based design pattern (Right); average of 40 earthquakes

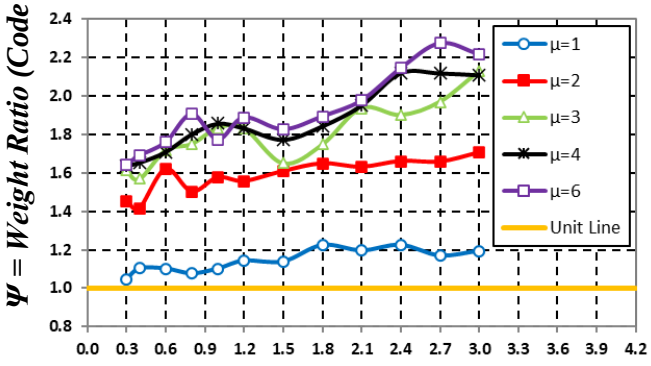

Figure 7. Structural weight ratio; the ratio of structural weight in code-based structures to that in optimum structure; average of 40 earthquakes

5. EFFECT OF OPTIMIZATION ON ENERGY-BASED REDUCTION FACTORS OF STRUCTURES

In force-based seismic design of structures, response modification factor or so-called strength reduction factor (R_s) is one of main parameters to incorporate the inelastic behaviour of the structures during an earthquake event [39, 46]. In fact, during a strong earthquake excitation, the total design strength recommended in seismic provisions are typically much lower than the total elastic base shear strength. Strength reductions from the elastic strength demand are prevalently accounted for through the use of strength reduction factor, R_s, which is one of the most controversial issues in the seismic-resistant design provisions. This factor, strongly dependent on the energy dissipation capacity of the structural systems, is used to reduce the elastic design force spectra in earthquake-resistant design while the recommended values could be to a large extent based on judgments, experiences and observed behaviors of structures during past earthquake events rather than analytical results. Similarly, in energy-based seismic design, the energy-based reduction factor (R_{EI}) for an MDOF system with specified fundamental period of vibration is defined as the total elastic input energy normalized, $EI_e(\mu=1)$, to the total inelastic input energy corresponding to the target inter-story ductility ratio, $EI_y(\mu=\mu_t)$, which can be written as:

$$R_{EI}=\frac{EI_e(\mu=1)}{EI_y(\mu=\mu_t)} \tag{16}$$

To examine the effect of optimization on energy-based reduction factor, the mean of R_{EI} spectra for both optimum based and code-based structures subjected to 40 selected earthquake ground motions for different ductility ratios of 2, 3, 4 and 6 are computed as shown in Fig. 8. It is observed that the energy-based reduction factors (R_{EI}) for short-period optimum structures with T≤ 0.6 s and long-period structures are always lower and greater than those for code-based structures, respectively. The differences are intensified by increasing the level of inelasticity such that in long-period optimum structures with high level of inelastic behavior (μ= 6) the values of R_{EI} are up to 30% greater than those in code-based structures. Conversely, in short-period optimum structures the values are up to 27% lower than code-based ones. As already discussed and shown in Fig. (6-a), the reason is referred to the difference between the inelastic input energies of optimum and code-based structures as the imparted energies in elastic range of response are nearly equal in both methods. Another point is that in velocity sensitive region (T> 0.6), R_{EI} increases with ductility demand while it decreases in acceleration sensitive region (T≤ 0.6). Hence, one may conclude that forced-based strength reduction factor and energy-based reduction factor have different relationship with inter-story ductility demand or inelastic behavior. In addition, using energy-based reduction factors of optimum structures in short-period and long-period regions can respectively overestimate and underestimate the required input energy demands for code-based structures, reflecting the difference dose exists in reality between the conventional forced-based methodology and energy-based seismic design

approach that can more realistically incorporate the frequency content and duration of earthquake ground motions.

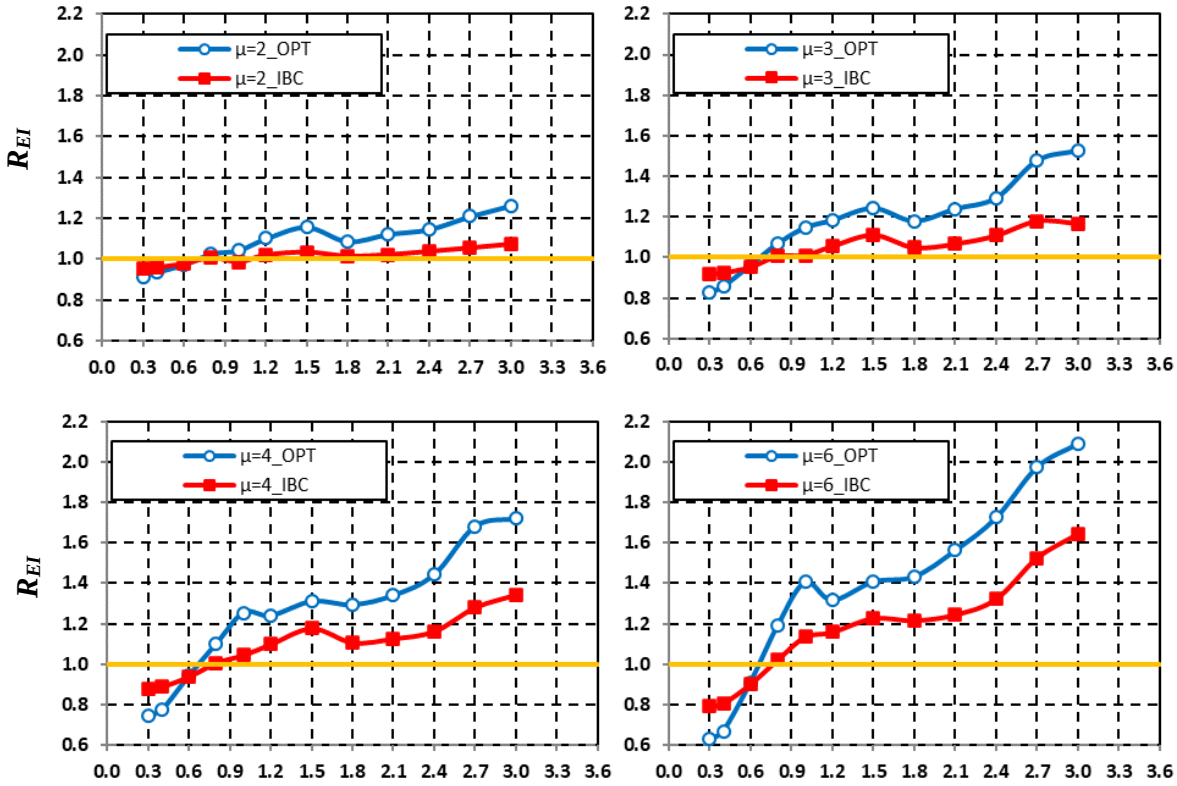

Figure 8. Energy-based reduction factors for optimum and code-based designs of structures; average of 40 earthquakes

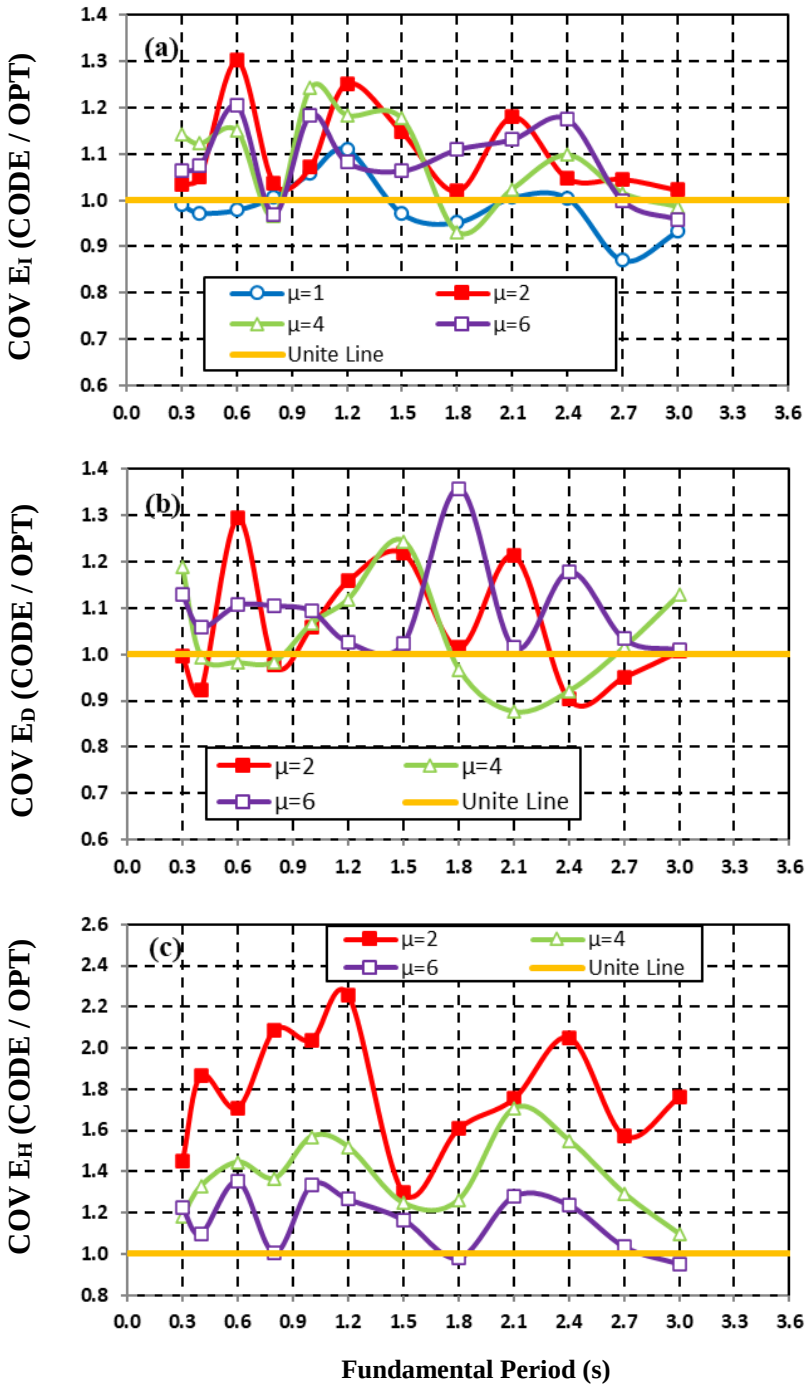

Figure 9. COV for optimum and code-based designs of structures; average of 40 earthquakes

6. DISPERSIONS OF ENERGY DEMANDS FOR OPTIMUM AND CODE-BASED DESIGNED STRUCTURES

To have more reliable results in nonlinear dynamic analysis of structure when subjected to a series of earthquake ground motions, it is always necessary to investigate the dispersion of results. In this section, the dispersions of the results for different energy parameters including input energy $COV(E_I)$, damping energy $COV(E_D)$ and yielding hysteretic energy $COV(E_H)$ are examined for both optimum and code-based structures through coefficient of variation (COV) of energy parameters. To better compare the results Fig. 9 is provided in such a way that the ratios of $COV(E_i)$, $COV(E_D)$ and $COV(E_H)$ in code-based model (CODE) to those in optimum structures (OPT) are computed and plotted. Fig. (9-a) shows that while no specific trend for different ductility demands is observed, except for some periods and elastic state, the ratio is larger than unity, indicating that the dispersion of the input energy results for code-based models are generally up to 30% greater than optimum structures. Similar to the input energy results, for damping energy cases also the dispersion for code-based structures is generally larger than optimum structures (Fig. 9-b). However, as shown in Fig. 8-c, the trend for hysteretic energy is completely different from input and damping energies such that the COV ratio are largely dependent on the level of inelastic behavior, and decreases as target ductility increases. The maximum value of $COV(E_H)$ ratio is observed for low inelastic behavior of 2 in which the dispersion of the results for code-based models is up to 2.26 times the optimum models. It can be concluded that, in general, the dispersions on results for energy parameters obtained from optimum designs are in average less than those for code-based frame counterparts, leading to more reliable results when compared to the conventional code-based structures.

7. CONCLUSION

In this study, the effects of optimization on seismic energy spectra including input energy, damping energy and yielding hysteretic energy are parametrically discussed. To this end, generic steel moment-resisting frames are optimized by using uniform damage and deformation approaches subjected to a set of 40 non-pule strong ground motions. Then, the maximum energy demand parameters are computed for different structures designed by optimum load pattern as well as code-based pattern. The results of this parametric study can be summarized as:

- In elastic range of response (μ=1), $E_I Ratio$ is in average independent of seismic load pattern, and optimization does not affect the elastic energy demand imparted to the structures. Nevertheless, when structures inter to the inelastic state, the ratio is remarkably influenced by the variation of the ductility ratio such that in short-period structures the energy values imparted to the optimum structures are larger (up to 21%) than those imparted to the code-based systems. After a threshold period (here T=0.6), the trend is reversed in such a way that the optimum designed structures take the input

energies much lower than the corresponding the code-based models, which are more intensified as the target ductility ratio increases.

- The values of $E_H Ratio$ are always significantly larger than unity, implying that the optimum structure can dissipate the seism input energy through inelastic behavior of their structural elements much more than its code-based designed structure counterpart. The maximum ratio is 2.56 for low inelastic behavior and reaches 1.2 for high level of inelastic response, μ=6. This phenomenon indicates that in optimum structures the seismic energy dissipation in each structural element is maximized and the material capacity is fully exploited. While the input energy demands of optimum structures are generally greater than code-based structures, the structural weight in optimum frames is much lower than that in structures designed by seismic code load pattern. It is seen that as ductility demand increases the structural weight ratio, defined as structural weight in code-based structures normalized by structural weight in the corresponding optimum structure, increases up to 2.2 for higher level inelastic behavior, demonstrating the efficiency of the proposed optimization approaches in seismic performance of building structures.
- Using energy-based reduction factors of optimum structures in short-period and long-period regions can respectively overestimate and underestimate the required input energy demands for code-based structures, reflecting the difference dose exists in reality between the conventional forced-based methodology and energy-based seismic design approach that can more realistically incorporate the frequency content and duration of earthquake ground motions.

The dispersions of the results for energy parameters obtained from optimum designs are in average less than those for code-based frame counterparts, leading to more reliable results when compared to the conventional code-based structures.

REFERENCES

1. ASCE/SEI 7-16. *Minimum Design Loads for Buildings and Other Structures*, American Society of Civil Engineers, Virginia, USA, 2016.
2. International Code Council. *International Building Code 2015*, Country Club Hills, IL, International Code Council, Inc, 2015.
3. EuroCode 8. *Design of structure for earthquake resistance – Part 1*: General rules for buildings. Bruxelles: European Committee for Standardization, 2004.
4. Standard No. 2800. *Iranian Code of Practice for Seismic Resistant Design of Buildings*, 4th Edition, 2013.
5. FEMA 356. *Prestandard and Commentary for the Seismic Rehabilitation of Buildings*, Federal Emergency Manage Agency, prepared by the American Society of Civil Engineers, Washington, D.C., 2000.
6. Smith RSH, Tso WK. Inconsistency of Force-Based Design Procedure, *J Seismol Earthq Eng* 2002; **4**(1): 46-54.
7. FEMA 440. *Improvement of Nonlinear Static Seismic Analysis Procedures*, Redwood City, 2005.

8. Hernandez-Montes E, Kwon O, Aschheim MA. An Energy Based Formulation for First and Multiple Mode Nonlinear Static (Pushover) analysis, *J Earthq Eng* 2004; **8**(1): 69-88.
9. Housner GW. Characteristics of Strong-Motion Earthquakes, *Bullet Seismol Society America* 1947; **37**(1): 19-31.
10. Housner GW. Limit design of structures to resist earthquakes, *Proceedings of the 1st World Conference on Earthquake Engineering California USA*, 1956, pp. 1-13.
11. Kato B, Akiyama H. Seismic design of steel buildings, *J Struct Div*, ASCE 1982; **108**(ST8): 1709-21.
12. Zahrah TF, Hall WJ. Earthquake energy absorption in SDOF structures, *J Struct Eng ASCE* 1984; **110**(8): 1757-72.
13. Bertero VV, Uang CM. *Implications of Recorded Earthquake Ground Motions on Seismic Design of Building Structures,* Research Report, UCB/EERC-88/13, University of California at Berkeley, 1988.
14. Uang CM. Comparison of Seismic Force Reduction Factors Used in USA and Japan, *Earthq Eng Struct Dyn* 1990; **20**(4): 389-97.
15. Uang CM, Bertero VV. Evaluation of Seismic Energy in Structures, *Earthq Eng Struct Dyn* 1990; **19**(1): 77-90.
16. Kuwamura H, Kirino Y, Akiyama H. Prediction of Earthquake Energy Input from Smoothed Fourier Amplitude Spectrum, *Earthq Eng Struct Dyn* 1993; **23**(10): 1125-37.
17. Bruneau M, Wang N. Some aspects of energy methods for the inelastic seismic response of ductile sdof structures, *Eng Struct* 1996; **18**(1): 1-12.
18. Yei L. Otani S. Maximum seismic displacement of inelastic systems based on energy concept, *Earthq Eng Struct Dyn* 1999; **28**: 1483-99.
19. Chou CC, Uang CM. Establishing absorbed energy spectra -an attenuation approach, *Earthq Eng Struct Dyn* 2000; **29**: 1441-55.
20. Chou CC, Uang CM. A procedure for evaluating seismic energy demand of framed structures, *Earthq Eng Struct Dyn* 2003; **32**: 229-44.
21. Adang S. Earthquake-resistant structural design through energy demand and capacity. *Earthq Eng Struct Dyn* 2007; **36**; 2099–2117. DOI: 10.1002/eqe.718
22. Leelataviwat S, Saewon W, Goel SC. Application of energy balance concept in seismic evaluation of structures, *J Struct Eng* 2009; **135**(2): 113-21.
23. Jiao Y, Yamada S, Kishiki S, Shimada Y. Evaluation of plastic energy dissipation capacity of steel beams suffering ductile fracture under various loading histories, *Earthq Eng Struct Dyn* 2011; **40**: 1553-70.
24. Ganjavi B, Hao H. A parametric study on the evaluation of ductility demand distribution in multi-degree-of freedom systems considering soil–structure interaction effects, *Eng Struct* 2012; **43**: 88-104.
25. Park K. Lateral load patterns for the conceptual seismic design of moment-resisting frame structures, Ph.D. Dissertation, University of Maryland, College Park, 2007.
26. Moghaddam H, Hajirasouliha I. Optimum strength distribution for seismic design of tall buildings, *Struct Des Tall Special Build* 2008; **17**(2): 331-49.

27. Goel SC, Liao WC, Reza Bayat M, Chao SH. Performance-based plastic design (PBPD) method for earthquake-resistant structures: an overview, *Struct Des Tall Special Build* 2010; **19**(1-2): 115-37.
28. Hajirasouliha I. Pilakoutas K. General seismic load distribution for optimum performance-based design of shear-buildings, *J Earthq Eng* 2012; **16**(4): 443-62.
29. Hajirasouliha I, Pilakoutas K, Reza K, Mohammadi RK. Effects of uncertainties on seismic behaviour of optimum designed braced steel frames, *Steel Compos Struct* 2016; **20**(2): 317-35.
30. Ganjavi B, Hao H. Optimum lateral load pattern for seismic design of elastic shear-buildings incorporating soil–structure interaction effects, *Earthq Eng Struct Dyn* 2013; 42(6): 913-33.
31. Ganjavi B, Hajirasouliha I and Bolourchi A. Optimum lateral load distribution for seismic design of nonlinear shear-buildings considering soil-structure interaction, *Soil Dyn Earthq Eng* 2016; **88**: 356-68.
32. Ogawa K, Kamura H, Inoue K. Modeling of moment resisting frame to fish-bone shape for response analysis, *J Struct Construct Eng (AIJ)* 1999; **521**: 119-26 (in Japanese).
33. Luco N, Mori Y, Funahashi Y, Cornell CA, Nakashima M. Evaluation of predictors of non-linear seismic demands using fishbone models of SMRF buildings, *Earthq Eng Struct Dyn* 2003; **32**(14): 2267-88.
34. Nakashima M, Ogawa K, Inoue K. Generic frame model for simulation of earthquake responses of steel moment frames, *Earthq Eng Struct Dyn* 2002; **31**(3): 671-92.
35. Kahloo AR, Khosravi H. Modified fish-bone model: A simplified model for simulation of seismic response of moment resisting frames, *Soil Dyn Earthq Eng* 2013; **55:** 195-20.
36. Medina RA, Krawinkler H. Strength demand issues relevant for the seismic design of moment-resisting frames, *Earthq Spectra* 2005; **21**(2): 415-39.
37. Esteva L, Ruiz SE. Seismic failure rates of multistory frames, *ASCE J Struct Eng* 1989; **115**(2): 268-84.
38. Fischinger M, Fajfar P, Vidic T. Factors contributing to the response reduction, *Proceedings of Fifth U.S. National Conference on Earthquake Engineering*, Chicago, Illinois, 1994, pp. 97-106.
39. Santa-Ana PR, Miranda E. Strength reduction factors for multi-degree of freedom systems, *Proceedings of the 12th World Conference on Earthquake Engineering*, Auckland, 2000.
40. Zareian F, Medina RA. A practical method for proper modeling of structural damping in inelastic plane structural systems, *Comput Struct* 2010; **88**(1-2): 45-53.
41. Park K, Medina RA. Conceptual seismic design of regular frames based on the concept of uniform damage, *J Struct Eng* 2007; **133**(7): 945-55.
42. Ganjavi B, Barania M, Hajirasouliha, I. Seismic Response Modification Factors for Stiffness Degrading Soil-Structure Systems, *Struct Eng Mech* 2018; **68**(2): 159-70.
43. Kaveh A. *Advances in Metaheuristic Algorithms for Optimal Design of Structures*, Springer International Publishing, Switzerland, 3rd edition, 2021.
44. OpenSees. Open system for earthquake engineering simulation, Version 2.6. Pacific Earthquake Engineering Research Center (PEER), 2016. http://opensees.berkeley.edu/

45. Chopra AK. *Dynamics of Structures, Theory and Application in Earthquake Engineering*, Pearson, 5th edition, 2016.
46. Eser M, Aydemir C, Ekiz L. Soil structure interaction effects on strength reduction factors, *Struct Eng Mech* 2012; **41**(3): 365-78.